International Journal of Automotive Technology, Vol. 12, No. 1, pp. 103–110 (2011)
DOI 10.1007/s12239–011–0013–0

1229–9138/2011/056–13

MODIFIED LATERAL CONTROL OF AN AUTONOMOUS VEHICLE BY LOOK-AHEAD AND LOOK-DOWN SENSING

T. Y. SHIN[1)], S. Y. KIM[1)], J. Y. CHOI[2)*], K. S. YOON[3)] and M. H. LEE[4)]

[1)]Department of Mechanical and Intelligent Systems Engineering, Pusan National University, Busan 609-735, Korea
[2)]Ulsan Automotive Parts Innovation Center, Ulsan Technopark, Ulsan 683-420, Korea
[3)]Division of Automotive, Industrial and Mechanical Engineering, Daegu University, Daegu 712-714, Korea
[4)]School of Mechanical Engineering, Pusan National University, Busan 609-735, Korea

(Received 19 April 2010; Rrevised 30 June 2010)

ABSTRACT–This paper presents a modified lateral control method for an autonomous vehicle with both look-ahead and look-down sensing systems. To cope with sensor noise and modeling uncertainty in the lateral control of the vehicle, a modified LMI-based H lateral controller was proposed, which uses the look-ahead information of the lateral offset error measured at the front of vehicle and the look-down information of the vehicle yaw angle error between the reference lane and the centerline of the vehicle. To verify the safety and the performance of the lateral control, a scaled-down vehicle was developed, and the positioning of the vehicle was estimated with USAT. The proposed controller, which uses both look-ahead and look-down information, was tested for lane changing and reference lane tracking with both simulation and experiment. The simulation and experimental results show that the proposed controller has better tracking and handling performance compared with a controller that uses only the look-ahead information of the target heading angle error.

KEY WORDS : Autonomous vehicle, Lateral control, LMI-based H control, Look-down information, Look-ahead information, USAT (Ultrasonic Satellite System), Scale-down vehicle

NOMENCLATURES

ψ_p : heading of the vehicle
υ : the lateral velocity of the vehicle at its C.G.
u : the longitudinal velocity of the vehicle at C.G.
δ : steering angle
m : the total mass of the vehicle
I_{zz} : the yaw moment of inertia
l : wheelbase of the vehicle
a/b : the distance from the vehicle's C.G. to the front/rear axles
a_y : the lateral acceleration of the vehicle
γ : the yaw rate of the vehicle
C_f/C_r : the front/rear cornering stiffnesses
L : look-ahead distance from the C.G. of the vehicle
ρ_{ref} : curvature of the reference lane
y_e : lateral offset error at the look-ahead position
ψ_e : vehicle's yaw angle error
β_T : target heading angle toward the target point
d_T : target distance
$r_T(i)$: the radius of the ith circular lane
$x_0(i)$: the initial x position of the ith lane in global coordinates
$y_0(i)$: the initial y position of the ith lane in global coordinates
$\psi_0(i)$: the starting yaw angle at the starting point of the ith lane
(x, y, z): the positions of the ultrasonic receivers
(x_i, y_i, z_i): the fixed position of the ith ultrasonic transmitter

*Corresponding author. e-mail: jychoi750@hotmail.com

1. INTRODUCTION

Recently, the automotive industry has focused on improving vehicle performance, safety and convenience for drivers. Intelligent transportation systems (ITSs) have been proposed to achieve such improvements, with applications including safety assistance for land vehicle drivers, unmanned transportation systems for goods in restricted areas, and unmanned surveillance systems. The other aim of ITSs is to achieve congestion-free and accident-free highways by maximizing the capacity of highways and minimizing driver-oriented accidents, which are known to be the main source of car accidents.

Autonomous vehicle systems have two basic control tasks: longitudinal control and lateral control. Longitudinal control is used for actions such as joining a fleet, splitting from it, and regulating the speed to maintain proper spacing between vehicles. Lateral control, or lanekeeping, is used to autonomously guide the vehicle along reference trajectories. Various lateral control algorithms have been proposed that use the relative lateral offset and heading of vehicles (Tan *et al*., 1999; Tsugawa, 1994; Choi *et al*.,

2002; Rossetter *et al*., 2004). A robust lateral controller was designed against variations in velocity, mass, and road-tire contact (Ackermann *et al*., 1995). These intelligent vehicle systems have been applied to buses and other transportation vehicles (Fritz, 1999; Hunt *et al*., 2000) in routine roadways. In the research of Makela and Numers (2001), an autonomous guided outdoor vehicle was developed to transport heavy steel slabs in a steel plant area. Ackermann *et al*. (1995) designed a robust controller to prevent vehicles from skidding due to wind and changes in the road condition.

The references and the sensing systems on roadways are classified as either active or passive (Tsugawa, 1999). They are also classified into systems that detect references in front of vehicles (look-ahead sensing) and those that detect references beneath vehicles (look-down sensing). Look-ahead sensing can be realized using vision sensors. Look-down sensors are classified as continuous or discontinuous. They can be realized with electrified wires, radar reflection, or buried permanent magnets. Each sensing scheme has its own advantages and disadvantages. Vision sensors have the advantage of look-ahead, which makes closed-loop control systems more stable. Efforts at Carnegie Mellon University (CMU), the National Institute of Standards and Technology (NIST), and in Germany have yielded promising experimental results using neural networks and classical vision algorithms. Vehicles that use the lane recognition algorithm are controlled using a new Levenberg-Marquardt neural network algorithm (Lee *et al*., 2002). However, acquiring and processing the optical images requires expensive equipment, and processing the optical images into credible data in real-time in all weather and road conditions is difficult. On the other hand, look-down sensing schemes that use either electrified wires or permanent magnets can be realized with inexpensive sensors and simple data processing and are guaranteed to work well in any weather and road conditions, but these schemes give no indications about the upstream road conditions, and the construction of the required infrastructure on the road can become expensive.

In conventional lateral control, the lateral control algorithm based on a non-slip model (Tsugawa, 1994, 1999) cannot be used when vehicle side-slip occurs. Kim *et al*. (2007) introduced a lateral PID controller to minimize the target heading angle and modified it with a heading angle modulator. An LMI-based H control that utilizes only the look-ahead information of the target heading angle error (Kim *et al*., 2006) was used to design a robust lateral controller against high frequency sensor noise and the modeling uncertainty from the variation of the longitudinal velocity, where the input and output weighting functions are designed according to the time domain performance specifications. In this paper, to reduce tracking errors and to improve tracking and handling performance, a modified LMI-based H lateral controller was proposed that utilizes the look-ahead information of the lateral offset error measured at the front of vehicle and the look-down information of the vehicle yaw angle error between the reference lane and the centerline of the vehicle. The safety and performance of the proposed lateral controller are verified by simulation and experiments using a scaled-down vehicle.

2. LATERAL CONTROL ALGORITHM

2.1. Reference Lane Construction

Reference lanes are constructed simply by a combination of straight lanes and circular lanes (Kim *et al*., 2006). One segment of a lane is represented by

$$\mathrm{Ref}_i=\{r_T(i),\ x_0(i),\ y_0(i),\ \psi_0(i)\} \tag{1}$$

In contrast with a mobile robot, a vehicle cannot always pass over the reference lane due to side slip and steering limitations. Thus, the ith segment of the reference lane is switched to the next i+1th segment, when the distance, d_{i+1}, between the next starting point, T_{i+1}, and the current point, (x_p, y_p), is smaller than D_1 as shown in Figure 1(a). The other case of switching is fulfilled when the distance, d_{i+1}, is increased relative to the previous distance, which prevents a vehicle from diverging, as shown in Figure 1(b).

As a result, the segment is switched to either

$$d_{i+1}\le D_1 \quad \text{or} \quad [d_{i+1}]_k \ge [d_{i+1}]_{k-1}+D_2 \tag{2}$$

where the subscript k is the time sequence and D_2 is a constant.

Figure 2 shows the reference lane information for the given L, where the target heading angle error β_e is obtained as

$$\beta_e=\tan^{-1}\left(\frac{y_e}{L}\right) \tag{3}$$

In an absolute positioning system, such as a global or local positioning system, the vehicle's position, (x_p, y_p), and

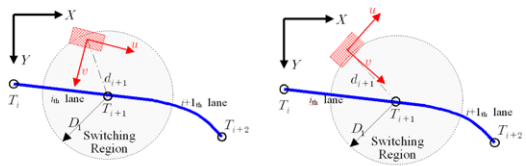

(a) Switching case 1 (b) Switching case 2

Figure 1. Segment switching in the reference lane.

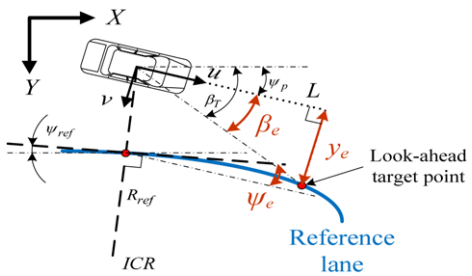

Figure 2. Look-ahead and look-down information from reference lane.

the vehicle's yaw angle, ψ_p, can be measured directly.

Then the target distance is described by

$$d_T=\sqrt{(L-x_p)^2+(y_e-y_p)^2} \tag{4}$$

In Figure 2, due to the motion of the vehicle and the change of the lane geometry, the equations capturing the evolution of lateral offset error, y_e, and the vehicle's yaw angle error, ψ_e, at the look-ahead distance, L, are given by

$$\begin{aligned}\dot{y}_e&=v+u\cdot\psi_e+L\cdot\gamma\\ \dot{\psi}_e&=\gamma-u\cdot\rho_{ref}\end{aligned} \tag{5}$$

where $\rho_{ref}=1/R_{ref}$ is the curvature of the reference lane (Ackermann *et al*., 1995).

2.2. LMI-Based H Control

An LMI-based H control (Kim *et al*., 2006) is introduced to design a robust lateral controller that performs stably against high frequency sensor noise and modeling uncertainty. The advantage of using weighted performance specifications is obvious in multi-variable system design (Zhou and Doyle, 1998). In the first place, some components of a vector signal are usually more important than others. In the second place, each component of the signal may not be measured in the same units. Therefore, weighting functions are essential to make these components comparable. To reject errors in a certain frequency range, some frequency-dependent weights must be chosen. The selection of weighting functions for a specific design problem often involves ad hoc fixing, much iteration, and fine tuning. It is difficult to give a general formula for weighting functions that will work in every case. Based on the time domain performance specifications, the corresponding requirements in the frequency domain, in terms of the bandwidth ω_b and the peak sensitivity M_s, can be determined. A possible choice of W_e can be obtained by modifying the weighting function as follows (Zhou and Doyle, 1998).

$$W_e=\frac{s/M_s+\omega_b}{s+\omega_b\varepsilon} \tag{6}$$

The magnitude of $|KS|$ in the low-frequency range is essentially limited by the allowable cost of the control effort and the saturation limit of the actuators; hence, in general, the maximum gain M_u of can be fairly large, while the high-frequency gain is essentially limited by the controller bandwidth (ω_{bc}) and the sensor noise frequencies. A candidate weight W_u would be for a small $\varepsilon_1>0$. The weighting for MIMO problems can be initially chosen as diagonal matrices, with each diagonal term chosen as shown above.

$$W_u=\frac{s+\omega_{bc}/M_u}{\varepsilon_1 s+\omega_{bc}} \tag{7}$$

2.3. Lateral Control with the Look-ahead Information

In the previous studies of Kim *et al*. (2006) and Kim *et al*. (2007), the basic algorithm for lateral control is to minimize the target heading angle error, β_e, at the look-ahead target point, as shown in Figure 3. As previously satisfied with the design specification for the H_∞ controller, the generalized plant is constructed, as shown in Figure 4. The nominal model, $P(s)$, is realized by the state vector $X_0=[v\ \gamma\ \psi_p]^T$, and the output vector $Y_0=\psi_p$ is given as follows

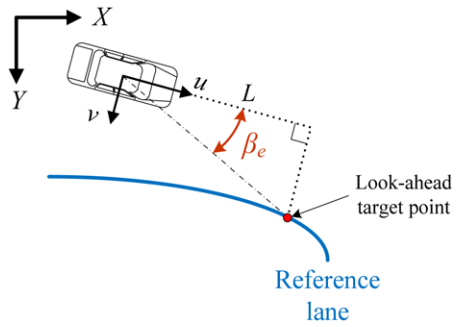

Figure 3. Lateral control algorithm utilizing the look-ahead information.

$$\begin{aligned}\dot{X}_0&=A_0X_0+B_0\delta\\ Y_0&=C_0X_0\end{aligned} \tag{8}$$

where,

$$A_0=\begin{bmatrix}-2(C_f+C_r)/mu & -u-2(aC_f-bC_r)/mu & 0\\ -2(aC_f-bC_r)/I_zu & -2(a^2C_f+b^2C_r)/I_zu & 0\\ 0 & -1 & 0\end{bmatrix},$$

$$B_0=\begin{bmatrix}2C_f/m\\ 2aC_f/I_z\\ 0\end{bmatrix}\ \text{and}\ C_0=\begin{bmatrix}0 & 0 & 1\end{bmatrix}$$

In Figure 4, $W_u(s)$ and $W_e(s)$ are the weighting functions for the input and the output and are realized by

$$G_0(s)=\begin{bmatrix}A_0 & B_0\\ C_0 & D_0\end{bmatrix},\ W_e(s)=\begin{bmatrix}A_e & B_e\\ C_e & D_e\end{bmatrix} \tag{9}$$

$$\text{and}\ W_u(s)=\begin{bmatrix}A_u & B_u\\ C_u & D_u\end{bmatrix}$$

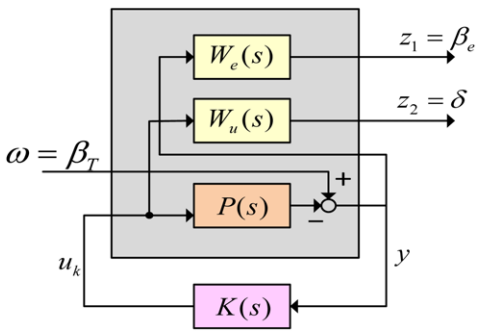

Figure 4. Generalized plant for lateral control with look-ahead information.

$K(s)$ is the designed H controller. The target heading angle β_T is defined as the external input ω.

The control objectives z_1 and z_2 represent the target heading angle error β_e and the steering angle δ.

Then, the generalized plant can be represented as the state space model below.

$$\begin{aligned}\dot{X} &= \begin{bmatrix} A_e & 0 & -B_eC_0 \\ 0 & A_u & 0 \\ 0 & 0 & A_0 \end{bmatrix} X + \begin{bmatrix} B_e \\ 0 \\ 0 \end{bmatrix} \beta_T + \begin{bmatrix} 0 \\ B_u \\ B_0 \end{bmatrix} \delta \\ Z &= \begin{bmatrix} C_e & 0 & -D_eC_0 \\ 0 & C_u & 0 \end{bmatrix} X + \begin{bmatrix} D_e \\ 0 \end{bmatrix} \beta_T + \begin{bmatrix} 0 \\ D_u \end{bmatrix} \delta \\ Y &= \begin{bmatrix} 0 & 0 & -C_0 \end{bmatrix} X \qquad + [1]\beta_T \quad + [0]\delta \end{aligned} \tag{10}$$

2.4. Modified Lateral Control with Look-ahead and Look-down Information

The previous lateral control algorithm, which utilizes the look-ahead information of the target heading angle error, is capable of coping with the change of lane curvature. However, when the look-down information is used, the tracking performance is disregarded. To reduce the lateral error and to improve riding feel at the same time, the controller is designed to minimize the look-ahead information of the lateral offset error, y_e, measured at the front of vehicle and the look-down information of the vehicle's yaw angle error, ψ_e, between the reference lane and the centerline of the vehicle, as shown in Figure 5. By fusing the look-ahead information and the look-down information, this modified control algorithm can be implemented. Here, the errors are also minimized with the LMI-based H control algorithm.

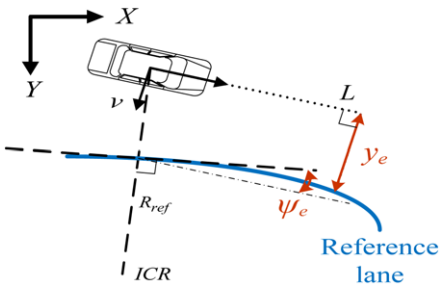

Figure 5. Modified lateral control algorithm utilizing the look-ahead and look-down information.

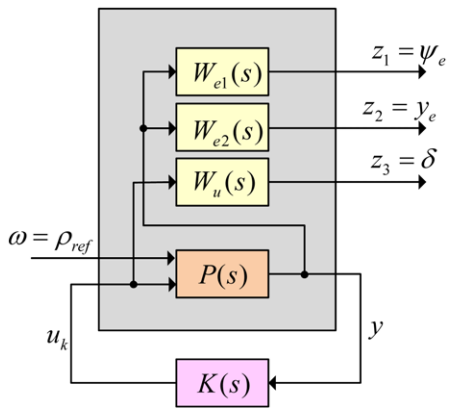

Figure 6. Generalized plant for the modified lateral control with look-ahead and look-down information.

By combining the two d.o.f. vehicle dynamics and the lane geometry, a state space model for the state vector $Y_0=[\psi_e\ y_e]^T$ is written as

$$\begin{aligned}\dot{X}_0 &= A_0X_0 + B_{01}\delta + B_{02}\rho_{ref} \\ Y_0 &= C_0X_0 \end{aligned} \tag{11}$$

where

$$A_0 = \begin{bmatrix} -2(C_f+C_r)/mu & -u-2(aC_f-bC_r)/mu & 0 & 0 \\ -2(aC_f-bC_r)/I_{zz}u & -2(a^2C_f+b^2C_r)/I_{zz}u & 0 & 0 \\ 0 & -1 & 0 & 0 \\ 1 & L & u & 0 \end{bmatrix}$$

$$B_{01} = \begin{bmatrix} 2C_f/m \\ 2aC_f/I_{zz} \\ 0 \\ 0 \end{bmatrix}, \quad B_{02} = \begin{bmatrix} 0 \\ 0 \\ u \\ 0 \end{bmatrix} \text{ and}$$

$$C_0 = \begin{bmatrix} 0 & 0 & 1 & 0 \\ 0 & 0 & 0 & 1 \end{bmatrix}$$

The external input ω is the curvature of the reference lane ρ_{ref}, which is treated as a disturbance.

The control objectives z_1, z_2, and z_3 represent the vehicle's yaw angle error ψ_e, the lateral offset error y_e, and the steering angle δ.

The generalized plant, as shown in Figure 6, can be represented as the state space model below.

$$\begin{aligned}\dot{X} &= \begin{bmatrix} A_{e1} & 0 & 0 & B_{e1}[10]C_0 \\ 0 & A_{e2} & 0 & B_{e2}[01]C_0 \\ 0 & 0 & A_u & 0 \\ 0 & 0 & 0 & A_0 \end{bmatrix} X + \begin{bmatrix} 0 \\ 0 \\ B_u \\ B_{01} \end{bmatrix} u_k + \begin{bmatrix} 0 \\ 0 \\ 0 \\ B_{02} \end{bmatrix} \rho_{ref} \\ Z &= \begin{bmatrix} C_{e1} & 0 & 0 & D_{e1}C_0 \\ 0 & C_{e2} & 0 & D_{e2}C_0 \\ 0 & 0 & C_u & 0 \end{bmatrix} X \quad + \begin{bmatrix} 0 \\ 0 \\ D_u \end{bmatrix} u_k + \begin{bmatrix} 0 \\ 0 \\ 0 \end{bmatrix} \rho_{ref} \\ Y &= \begin{bmatrix} 0 & 0 & 0 & C_0 \end{bmatrix} X \qquad\qquad + [0]u_k \quad + [0]\rho_{ref} \end{aligned} \tag{12}$$

3. VEHICLE AND ULTRASONIC SATELLITE SYSTEM

3.1. Configuration of the Scaled-down Vehicle

Figure 7 shows a 1/10 scaled-down vehicle, the wheel base and mass are 0.285 m and 2.105 kg, respectively. Two wheel drive and two wheel steering are adopted. The maximum speed of the vehicle is 1.2 m/s. The maximum steering angle is 30°. The specification of the scaled-down vehicle, except for speed, is a reasonable representation of a real vehicle, such as a sedan or a small-sized jeep. For the

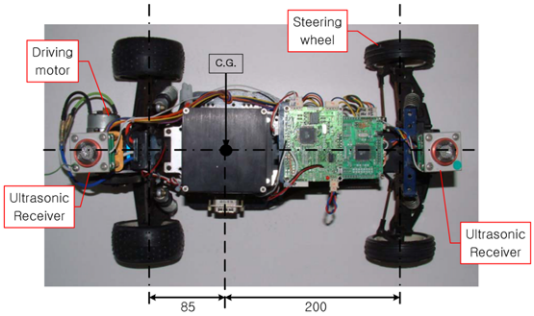

Figure 7. Scaled-down vehicle.

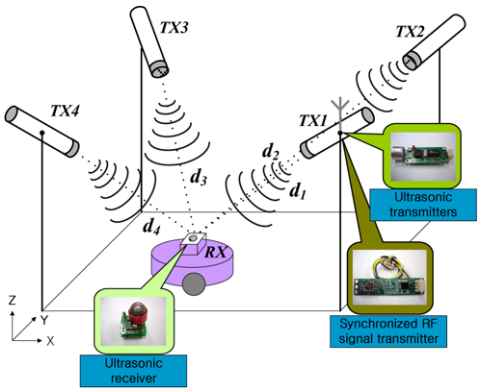

Figure 8. Configuration of USAT.

positioning of the scaled-down vehicle, the USAT (Ultrasonic Satellite System) is used (Lee *et al*., 2007a). The information about vehicle's position and yaw angle and TOFs is sent to a remote-control system by a wireless communication system with RS-232. The remote-control system judges the position and re-transmits the driving and steering commands to a CPU attached to the scaled-down vehicle.

Lee *et al*. (2007b) elaborated a 3D ultrasonic local positioning system, USAT, equipped a 40 kHz transmitter/receiver of direct ultrasonic waves, as shown in Figure 8. A 40 kHz ultrasonic transmitter with roughly 3 kHz of bandwidth is used. Considering the directive angles of the transmitter and the receiver, if the transmitters are attached at 45°, the recognizing region is defined.

The procedure for positioning by USAT is as follows. After sending ultrasonic wave and RF signals synchronously to the fixed transmitting-part as a pseudo-satellite, the receiving-part attached to a movable object acquires them. The distance information is then resent to a remote-control. Finally, the position is determined by the remote-control.

3.2. Ultrasonic Satellite System

In this paper, a period-detecting technique is used to find the time of flight of the ultrasonic waves (Lee *et al*., 2007a or b?). Comparing the results of the threshold-detecting technique (Wehn and Belanger, 1997), the proposed technique has no problem with measuring distances under 30 m. USAT, similar to the GPS, locates the position by using the elapsed time from the transmission to the reception of the wave.

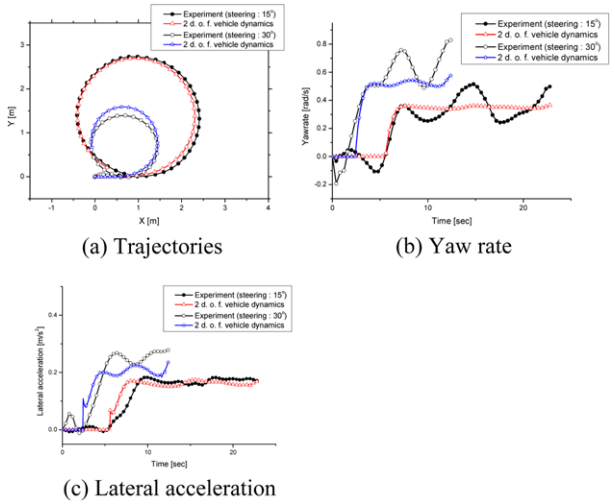

(a) Trajectories (b) Yaw rate

(c) Lateral acceleration

Figure 9. Parameter estimation results under

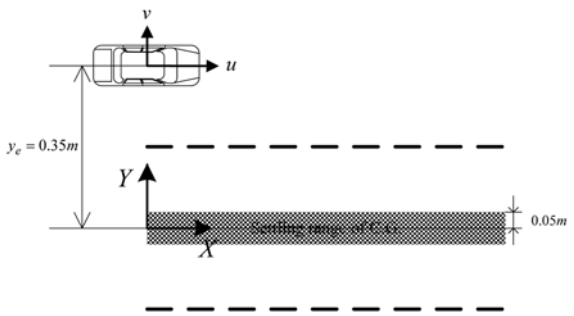

Figure 10. Settling range and initial position for lane change.

$$\begin{aligned}(x_1 - x_2)x + (y_1 - y_2)y + (z_1 - z_2)z &= \alpha \\ (x_2 - x_3)x + (y_2 - y_3)y + (z_2 - z_3)z &= \beta \\ (x_3 - x_4)x + (y_3 - y_4)y + (z_3 - z_4)z &= \gamma\end{aligned} \tag{13}$$

The positions of the ultrasonic receivers (x, y, z) can be calculated as follows, where (x_i, y_i, z_i) $(i=1, 2, 3, 4)$ are the positions of the four fixed ultrasonic transmitters and d_i $(i=1, 2, 3, 4)$ are the distances between transmitters and receivers.

Equation (13) can be written as

$$\begin{bmatrix} x \\ y \\ z \end{bmatrix} = A^{-1} \begin{bmatrix} \alpha \\ \beta \\ \gamma \end{bmatrix} \tag{14}$$

where $A = \begin{bmatrix} (x_1 - x_2) & (y_1 - y_2) & (z_1 - z_2) \\ (x_2 - x_3) & (y_2 - y_3) & (z_2 - z_3) \\ (x_3 - x_4) & (y_3 - y_4) & (z_3 - z_4) \end{bmatrix}$,

$$\alpha=\frac{1}{2}\{(x_1^2-x_2^2+y_1^2-y_2^2+z_1^2-z_2^2)-(d_1^2-d_2^2)\},$$
$$\beta=\frac{1}{2}\{(x_2^2-x_3^2+y_2^2-y_3^2+z_2^2-z_3^2)-(d_2^2-d_3^2)\},$$
$$\gamma=\frac{1}{2}\{(x_3^2-x_4^2+y_3^2-y_4^2+z_3^2-z_4^2)-(d_3^2-d_4^2)\}$$

Thus, the transmitters should be located so that the inverse matrix of A in Equation (14) may exist, that is, $\det A\neq 0$. The least-square estimator is used for the errors, which are linearly related to geometry (Lee *et al.*, 2007a or b?).

3.3. Vehicle Parameter Estimation and Verification

Parameters such as the mass, m, distance from the C.G. to the front and the rear axle, a and b, respectively, can be easily measured. However, it is difficult to measure the front and rear cornering stiffnesses, C_f and C_r, respectively, and the yaw moment of inertia, I_{zz}. The unknown parameters can be estimated by the least-square algorithm, as mentioned in the previous section. To estimate the parameters, Equation (8) is reconstructed as follows

$$\begin{aligned}&(2v+2a\gamma-2u\delta)\cdot C_f+(2v-2b\gamma)\cdot C_r=-(mu\dot{v}+mu^2\gamma)\\&u\dot{\gamma}\cdot I_{zz}+(2av+2a^2\gamma-2au\delta)\cdot C_f+(2b^2\gamma-2bv)\cdot C_r=0\end{aligned}\quad(15)$$

where the output is acquired by a J-turn test with a velocity of 0.5 m/s and 15° and 30° steering angles. Figure 9 shows the results of the parameter estimation, where the vehicle position is sensed by USAT. The main factor behind the mismatch in the results may be due to the nonlinearity of the tires, the limitation of wheel alignment or the steering delay (Choi *et al.*, 2002a or b?).

4. SIMULATION AND EXPERIMENT FOR THE LATERAL CONTROL

Both the controller that uses the look-ahead information and the modified controller that uses the look-ahead and down information are simulated and tested experimentally in lane change and the reference lane tracking scenarios. Both lateral controllers are designed and tuned with the LMI-based H_∞ control algorithm. The look-ahead distance is set at 0.5 m, and the segment switching distance, D_1, is 0.3 m. Because of the sensing range limitation of USAT, the vehicle speed is low (0.50 m/s), it cannot be driven until it achieves a steady state when changing lanes, and the curvature of the lane used for lane tracking is small (1.3 m). In the lane change maneuver, the scaled-down vehicle started with 0.35 m lateral offset and a 0 radian yaw angle with a speed of 0.35 m/s, as shown in Figure 10. A lane for reference lane tracking is given, as shown in Figure 11. The length of the straight lane is 2 m and the radius is selected to be 1.3 m to reflect the limitation of the indoor driving space and side slip under low velocity.

In both the controller that uses the look-ahead information and the modified controller that utilizes the look-ahead and look-down information, the control input weighting function is tuned by

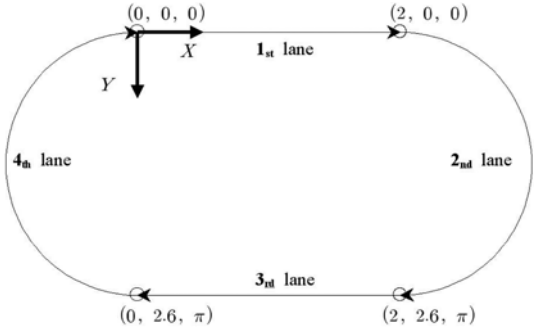

Figure 11. Reference lane for tracking.

$$W_u=\frac{s+0.4014}{0.001s+0.0.4014}\quad(16)$$

The error weighting functions for each controller are tuned by

$$W_{\beta_e}=\frac{s+15}{s+0.0015},\ W_{\psi_e}=\frac{0.5s+10}{s+0.001}\ \text{and}\ W_{y_e}=\frac{0.5s+5}{s+0.0005}.\quad(17)$$

4.1. Simulation Results

Figure 12 shows the simulation results of lane changing. As shown in Figure 12(a), both controllers are able to change the lane at a low velocity 0.35 m/s. Compared with the controller that uses only the look-ahead information, the modified controller has no overshoot, but the settling time of the controller that uses only the look-ahead information is smaller. Figure 12(b) shows that the modified

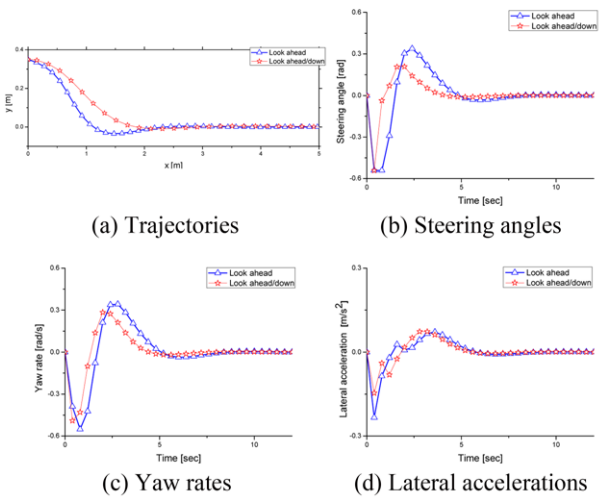

(a) Trajectories (b) Steering angles

(c) Yaw rates (d) Lateral accelerations

Figure 12. Simulation results of lane change maneuvering (u=0.35 m/s).

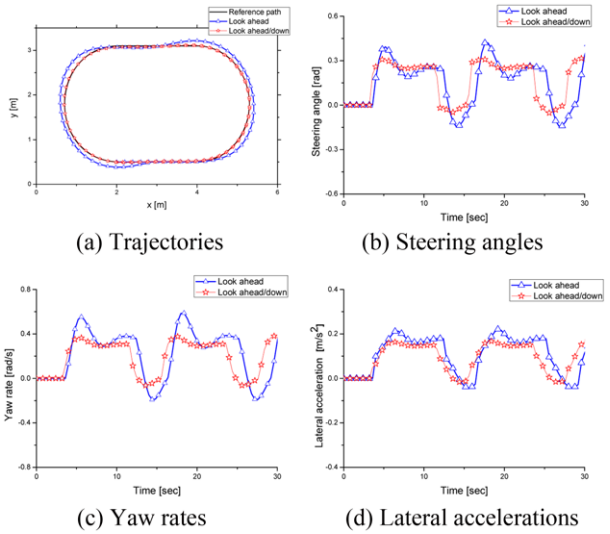

(a) Trajectories (b) Steering angles

(c) Yaw rates (d) Lateral accelerations

Figure 13. Simulation results of the lane tracking (u=0.50 m/s).

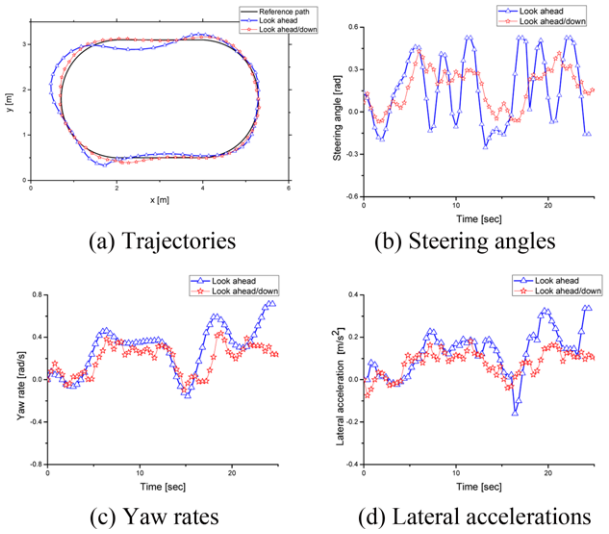

(a) Trajectories (b) Steering angles

(c) Yaw rates (d) Lateral accelerations

Figure 15. Experimental results of the lane tracking (u= 0.50 m/s).

controller has the advantage of a diminished control energy. Regarding the lateral motion of vehicle, the riding feel can be indicated by the yaw rate and lateral acceleration. Thus, the modified controller has better handling performance than the other controller, as shown in Figures 12(c), (d).

In the lane tracking simulation, the proposed controller gives better tracking performance and handling performance than the other controller, as shown in Figure 13. Generally, a lateral controller must achieve a compromise between tracking performance (settling time, lateral overshoot) and handling performance (yaw rate, lateral acceleration).

4.2. Experiment of Lane Change Maneuvering

Figure 14 shows the moving trajectories, steering angles, yaw rates, and lateral accelerations for the lane change experiment. In Figure 14(a), the trajectory of the vehicle using the modified controller performs more stably than the controller that uses only the look-ahead information.

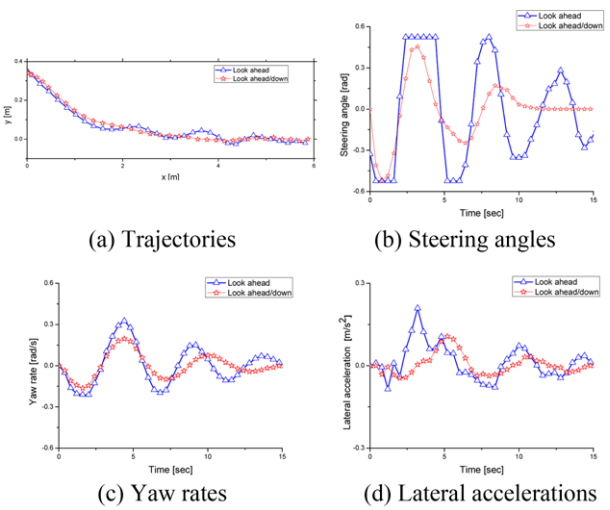

(a) Trajectories (b) Steering angles

(c) Yaw rates (d) Lateral accelerations

Figure 14. Experimental results of lane change maneuvering (u=0.35 m/s).

As shown in Figures 14(b)~(d), compared with the simulation results, the oscillation of response is increased in the experiment due to modeling error. However, the responses of the modified controller display better handling performance than the responses of the controller that utilizes only the look-ahead information. Thus, the experimental results of the lane change maneuvering are remarkably consistent with the simulation results.

4.3. Experiment of Reference Lane Tracking

For the given reference lane shown in Figure 11, the experimental results of lane tracking are shown in Figure 15. In Figure 15(a), compared to the simulation tracking errors, the experimental tracking errors are increased due to modeling error and sensor noise. However, the modified controller has a smaller tracking error than the other controller. Furthermore, the steering angle, yaw rate, and lateral acceleration of the modified controller demonstrate more stable performances than the other controller, as shown in Figure 15(b)~(d).

Additionally, the maximum value in steering angle, yaw rate, and lateral acceleration are caused by the discontinuity of lane curvatures from infinity (straight lane) to 1/1.3 (circular lane). In Figure 15, these experimental results are similar to the earlier lane tracking simulation results. Therefore, the proposed modified controller shows better tracking and handling performance than the controller that utilizes only the look-ahead information.

5. CONCLUSION

This paper presents a lateral control method for an auto-

nomous vehicle that uses both look-ahead and look-down information in an absolute positioning system. In the absolute positioning system, a reference lane was simply constructed by a combination of straight lanes and circular lanes. The reference lane can be constructed to prevent discontinuity of the reference command. To cope with sensor noise and modeling uncertainty in the lateral control of the vehicle, a modified LMI-based H_∞ lateral control was proposed that uses the look-ahead information of the lateral offset error measured at the front of vehicle and the look-down information of the vehicle yaw angle error between the reference lane and the centerline of the vehicle. By fusing the look-ahead information and the look-down information, the modified control algorithm can be implemented. To verify the safety and the performance of the lateral control, a scaled-down vehicle was developed, where the positioning of the vehicle was estimated using USAT. Based on the simulation and experiment results, the tracking error of the modified controller was reduced and it demonstrates better tracking and handling performance compared with the controller that utilizes only look-ahead information during lane changing and tracking.

REFERENCES

Ackermann, J., Guldner, J., Sienel, W., Steinhauser, R. and Utkin, V. I. (1995). Linear and nonliner controller design for robust automatic steering. *IEEE Trans. Control Systems Technology* **3**, **1**, 132–143.

Choi, J. Y., Hong, S. J., Park, K. T., Yoo, W. S. and Lee, M. H. (2002). Lateral control of autonomous vehicle by yaw rate feedback. *J. Mechanical Science and Technology* **16**, **3**, 338–343.

Fritz, H. (1999). Longitudinal and lateral control of heavy duty trucks for automated vehicle following in mixed traffic: Experimental results from the CHAUFFEUR project. *Proc. IEEE Int. Conf. Control Application*, 1348–1352.

Hunt, K. J., Johansen, T. A., Kalkkuhl, J., Fritz, H. and Gottsche, T. (2000). Speed control design for an experimental vehicle using a generalized gain scheduling approach. *IEEE Trans. Control Systems Technology* **8**, **3**, 381–395.

Kim, C. S., Kim, S. Y., Ryu, J. H. and Lee, M. H. (2006). LMI-based H_∞ lateral control of an autonomous vehicle by look-ahead sensing. *Int. J. Automotive Technology* **7**, **5**, 609–618.

Kim, S. Y., Lee, J.-M., Lee, D. H. and Lee, M. H. (2007). Unmanned navigation of vehicle using the ultrasonic satellite system. *J. Control, Automation, and Systems Engineering* **13**, **9**, 875–882.

Lee, D. H., Kim, S. Y., Yoon, K. S. and Lee, M. H. (2007a). A long range accurate ultrasonic distance measurement system by using period detecting method. *J. Korean Society for Precision Engineering* **24**, **8**, 41–49.

Lee, D. H., Kim, S. Y., Yoon, K. S. and Lee, M. H. (2007 b). USAT(Ultrasonic Satellite System) for the Autonomous Mobile Robots Localization. *J. Control, Automation, and Systems Engineering* **13**, **10**, 956–961.

Lee, K. B., Kim, Y. J., Ahn, O. S. and Kim, Y. B. (2002). Lateral control of autonomous vehicle using Levenberg-Marquardt neural network algorithm. *Int. J. Automotive Technology* **3**, **2**, 71–77.

Makela, H. and Numers, T. V. (2001). Development of a navigation and control system for an autonomous outdoor vehicle in a steel plant. *Control Engineering Practice*, **9**, 573–583.

Rossetter, E. J., Switkes, J. P. and Gerdes, J. C. (2004). Experimental validation of the potential field lanekeeping system. *Int. J. Automotive Technology* **5**, **5**, 95–108.

Tan, H. S., Guldner, J., Patwardhan, S., Chen, C. and Bougler, B. (1999). Development of an automated steering vehicle based on roadway magnets-A case study of mechatronic system design. *IEEE/ASME Transactions on Mechatronics* **4**, **3**, 258–272.

Tsugawa, S. (1994). Vision-based vehicles in Japan: Machine vision systems and driving control systems. *IEEE Trans. Industrial Electronics* **41**, **4**, 389–405.

Tsugawa, S. (1999). An overview on control algorithms for automated highway systems. *IEEE/IEEJ/JSAI Int. Conf.*, 234–239.

When, H. W. and Belanger, P. R. (1997). Ultrasound-based robot position estimation. *IEEE Trans. Robotics and Automation* **13**, **5**, 682–692.

Zhou, K. and Doyle, J. C. (1998). *Essentials of Robust Control.* Prentice-Hall International.